

Prediction of Flow Dynamic Features for River Nile Confluence Zone

Gamal El Saeed¹, Neveen Badway², Hossam Elsersawy³, Fatma Samir⁴

¹Professor of Hydraulics and Water Resources, Faculty of Engineering, Shobra, Benha University.

²Associate Professor, Faculty of Engineering, Shobra, Benha University.

³Associate Professor, Nile Research Institute, National Water Research Center.

⁴Researcher Assistant, Nile Research Institute, National Water Research Center.

Received 26 February 2020; Accepted 09 March 2020

Abstract

A confluence is a natural component in river and channel networks. The incoming flow from the tributary channel causes extensive variation of the flow velocity, flow discharge, turbulent intensity and sediment discharge in the main-channel. In the present paper, numerical model is applied to predict flow pattern and morphological changes at the future. The numerical model was calibrated using available confluence field data and then was applied to a confluence. The objectives of this study are to: evaluate the morphological changes at channel confluence, showing the behavior of the planform confluence morpho-hydro dynamics zones at the future, presenting the cumulative erosion and sediment at the study confluence and the rate of changes for the confluence hydrodynamic zone (CHZ) stagnation zone, separation zone, confluence scour, region of maximum velocity, region of flow recovery, and mixing interface/shear layer.

Key Words

Confluence, Hydro-dynamic Features, Nile River, Numerical Model and Prediction.

I. INTRODUCTION

River confluences play a major role in the routing of flow and sediment through fluvial systems. The hydrodynamic zone (CHZ) divided the flow into six zones and denoted them as follows: (i) a stagnation zone where flow velocity is reduced near the upstream junction corner; (ii) a flow separation zone at the downstream junction corner; (iii) a confluence scour; (iv) the maximum velocity/flow acceleration zone of the downstream channel; (v) flow recovery at the downstream end of the CHZ. and (vi) a shear layer/mixing interface between the two confluent flows. The key factors controlling the bed morphology, sediment transport, and flow pattern of the CHZ at simple confluences include planform symmetry, junction angle, momentum flux ratio, and bed concordance [Rhoads and Johnson, 2018].

Over the last 30 years, both laboratory and field experiments have provided valuable information on the morphology and flow dynamics of river junctions [Mosley, 1976; Ashmore, 1982; Reid et al., 1989; Best, 1987, 1988; Best and Roy, 1991; Biron et al., 1993a, 1993b; Gaudet and Roy, 1995; Biron et al., 1996a, 1996b; McLelland et al., 1996; De Serres et al., 1999; Rhoads and Kenworthy, 1995, 1998; Rhoads and Sukhodolov, 2001, 2004; Sukhodolov and Rhoads, 2001]. However, very few studies have examined sediment transport at those sites [Best, 1987, 1988]. Furthermore, the relation between sediment transport and the dynamics of the shear layer created at the interface between the two combining flows has not been described. Shear layers are characterized by high turbulence intensities and shear stresses and by the presence of well-organized flow structures [Winant and Brownand, 1974; Lee and Clark, 1980; Hussain and Zaman, 1985; Nezu and Nakagawa, 1993; Biron et al., 1996b; McLelland et al., 1996; De Serres et al., 1999; Sukhodolov and Rhoads, 2001; Rhoads and Sukhodolov, 2004]. The complexity of the flow in this zone has, however, generated many questions concerning the type and scale of the turbulent structures within this region and the processes responsible for their creation and dissipation [Best and Roy, 1991; Biron et al., 1993b; Rhoads and Sukhodolov, 2001, 2004]. Critically, this turbulence intensity may play an important role in the transport of sediment.

The principal objectives of the present study are: evaluate the morphological changes at channel confluence, showing the behavior of the planform confluence morpho-hydro dynamics zones at the future, presenting the cumulative erosion and sediment at the study confluence and the rate of changes for the hydrodynamic zones.

II. MATERIAL AND METHODS

2.1 Methodology

The methodology of this paper is: Review the literature and collecting the available field data such as bed levels flow velocity, properties of the bed particles and the passing discharge at the selected confluence. Collect the

field data including surveying the water surface profile and morphological changes due to different discharge conditions along the entire reach. Applying numerical model (Delft-3D) to get the hydraulic properties at the selected confluence at this time and future. The model is utilized to predict naturally morphological changes, including hydrodynamic features, to estimate the forces that influence the entrainment and deposition of individual particles.

2.2 Study area

An asymmetrical confluence at km 27 from El Roda gauge, near El Marzeek bridge was used for this study. This is an asymmetrical confluence, channelized confluence with a junction angle of 25°, momentum flux ratio 0.4 at maximum flow, and upstream channel widths (mean and tributary) of approximately 223m and 124m respectively, merging into a downstream channel of width 363m, at year 2016. There is bridge at 750m downstream the confluence (figure 1).

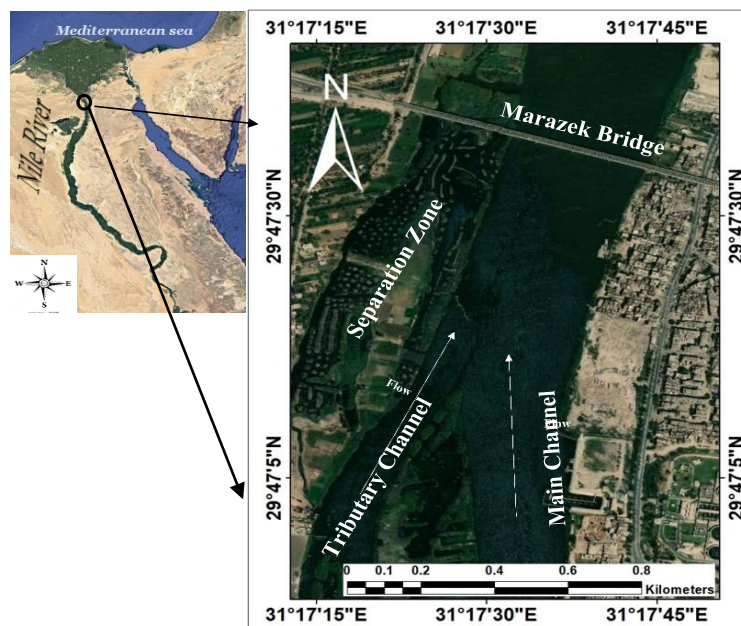


Figure 1: The study confluence and its location

2.2.1 Data collection

The bathymetric data were obtained from the contour maps, produced from the hydrographic survey of year 2016 provided by Nile Research Institute (NRI). Field measurements were conducted on a series of cross sections at the confluence in July 2019. Data were obtained from hydrodynamic measurements and bathymetric surveys by using Doppler current profiler (ADCP), the measured cross sections location shown at figure 2. The hydrological data presents water level and flow rate downstream Assuit Barrage. The daily monitoring of passing discharges through the located hydraulic structures (barrages) and the upstream and downstream corresponding water levels of those barrages as well as at different gauge stations is essential. Concerning study reach, two-gauge stations are located as shown in table 1.



Figure 2: ADCP data points along the study reach during the field measurements at year 2019

Table 1: Location of water level measuring stations

Gauge	Km from Gauge	
	El Roda	OAD
El Roda	0	927
Al Lathy	53.3	873.7

III. MODEL APPLICATION

2.2.2 Model description

A detailed numerical morphological model was setup using the numerical software package Delft-3D, which was developed by Deltares for multi-approaches; where it can carry out simulations of flows, sediment transports, waves, water quality, particle tracking, morphological developments and ecology, **DELTA RES (2014a)**. The primary purpose of the computational model Delft3D is to solve various one-, two- and three-dimensional, time-dependent, non-linear differential equations related to hydrostatic and non-hydrostatic free-surface flow problems. Delft3D-FLOW solves the Navies Stokes equations for an incompressible fluid, under the shallow water and the Boussinesq assumptions. In the vertical momentum equation, the vertical accelerations are neglected, which leads to the hydrostatic pressure equation.

For reliable hydrodynamic computations the grid should fulfill the requirements of smoothness, orthogonality, and should have an aspect ratio close to unity (see Thompson et al., 1985; Wijnbenga, 1985; and Mosselman, 1991). A fine unstructured grid (5 m*5 m) consisting of 145587 nodes was created.

2.2.3 Boundary Condition

The model was calibrated from year 2016 to year 2019. To predict the hydrodynamic features the model was run as a time series of the last ten years from year 2019 to year 2029. Figures 4&5 show the time series (discharge and corresponding water level) used for calibrate the model and time series from year 2019 to 2029 used to prediction case. Survey of year 2016 is used.

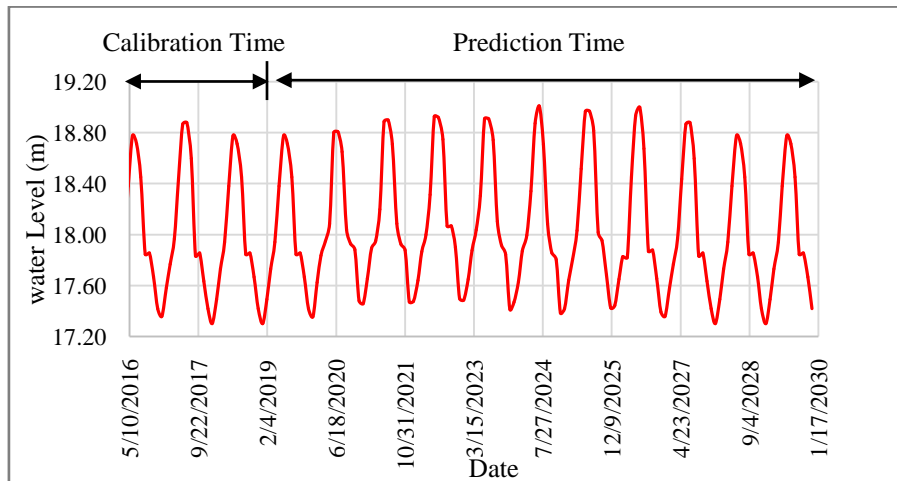


Figure 4: The used water level from year 2016 to year 2029 at the study confluence

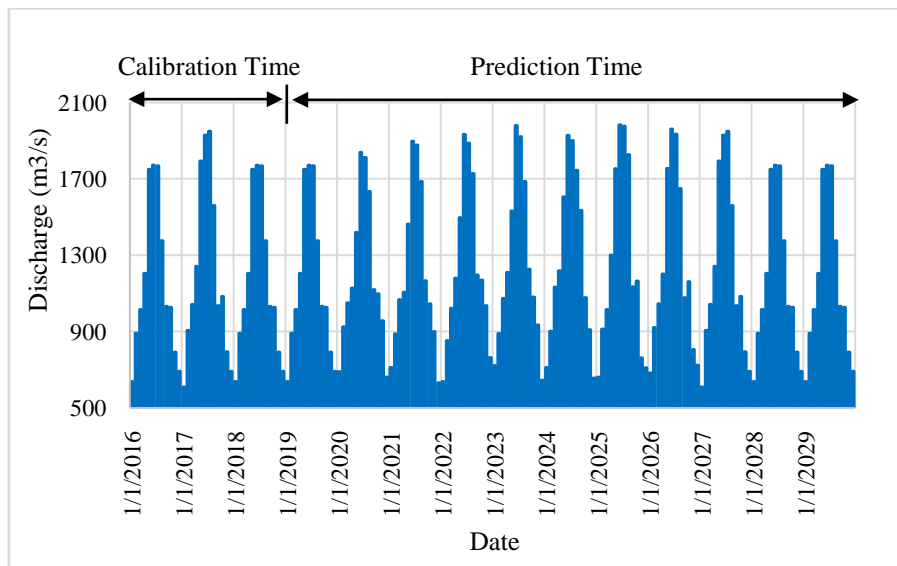


Figure 5: The corresponding discharge from year 2016 to year 2029 at the Assuit barrage

2.2.4 Model calibration

The model was run from year 2016 to 2019 and the results were compared with measured field data at year 2019 (with discharges of 1930 m³/s and corresponding water level 18.80 m), on average velocity, and bed elevation. The model output showed that the simulation of water levels and bed elevation was highly accurate as shown at figures 6 and 7. Manning roughness coefficient (n) was defined at each grid point, and ranged from 0.025 to 0.035. The morphology of the fractions was computed using the “Meyer-Peter-Muller (1948)” sediment transport predictor formula.

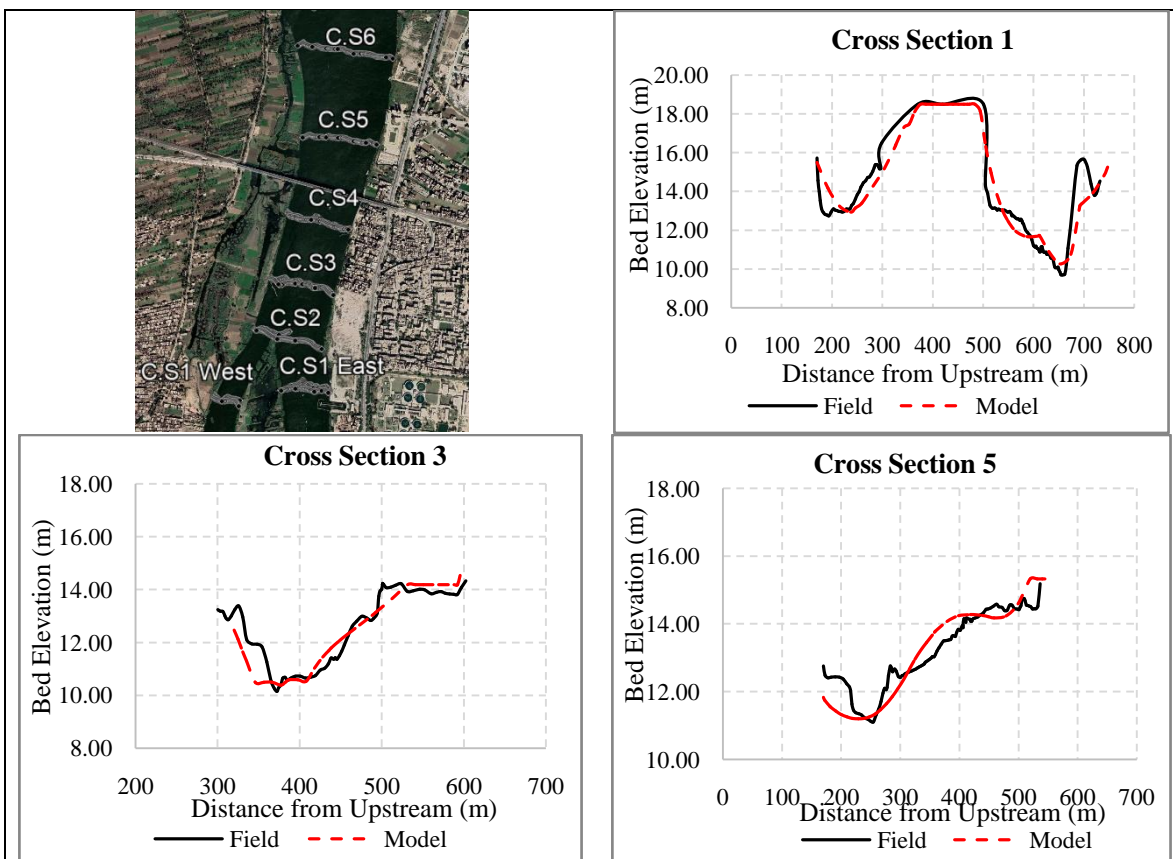
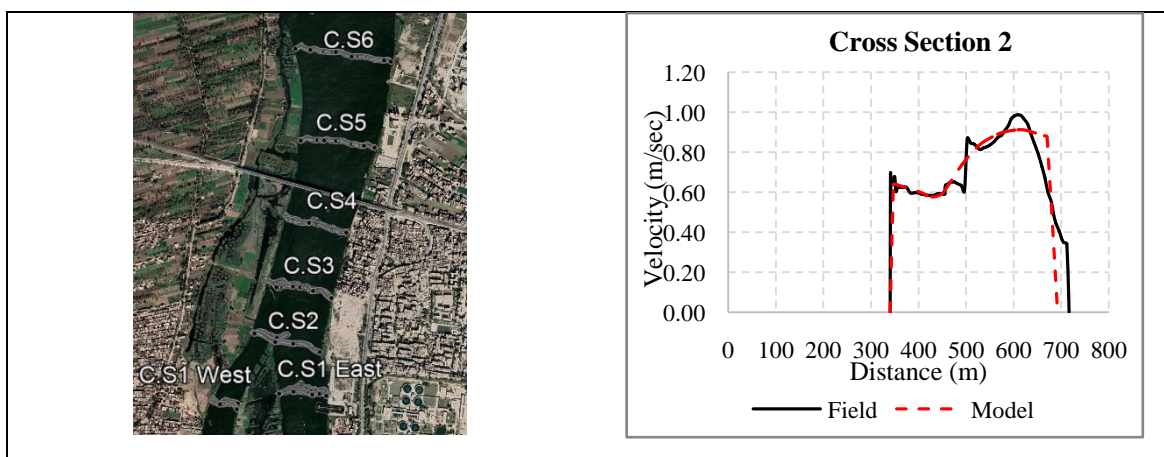


Figure 6: Comparison of measured and predicted bed elevations at year 2019 and the cross sections location



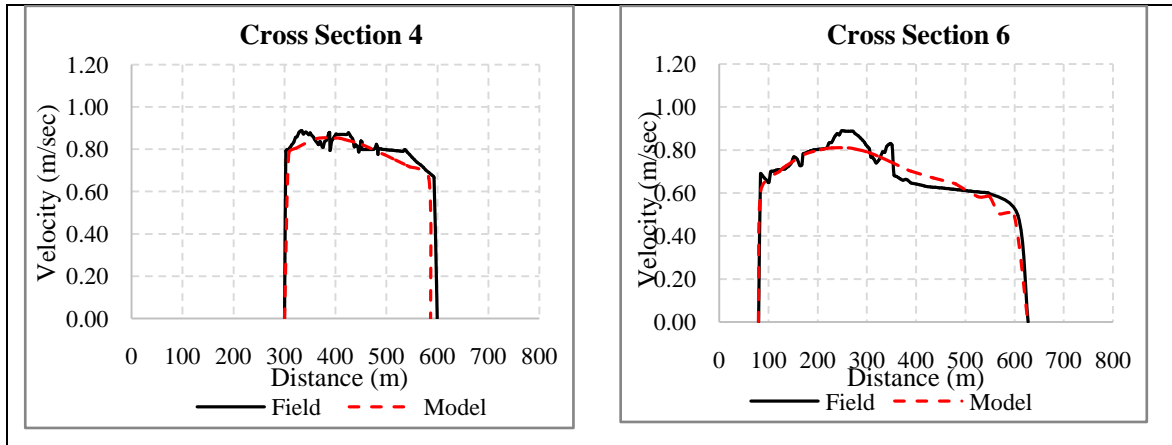
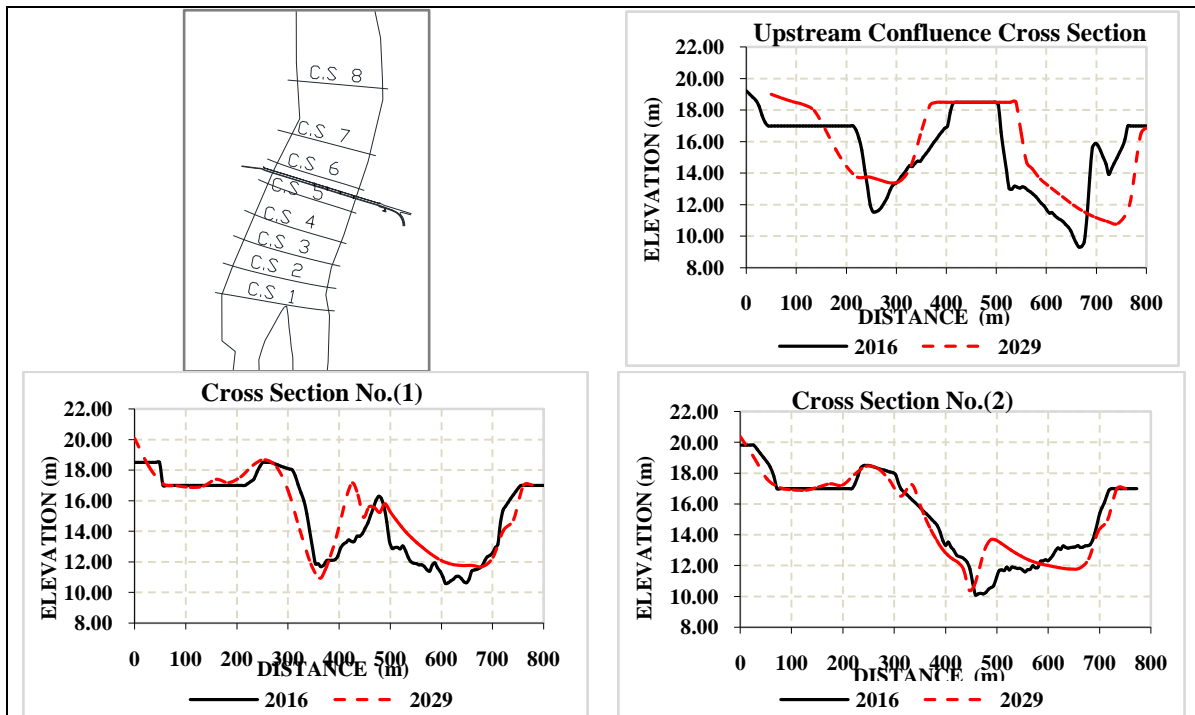


Figure 7: Comparison of measured and predicted depth average velocity at year 2019 and the cross sections location

IV. RESULTS AND ANALYSIS

2.2.5 Confluence morphological changes

The model was utilized to predict naturally morphological changes, including hydrodynamic features. Figure 8 shows the reach bed elevation at years 2016 and 2029, one cross section upstream and eight cross sections downstream the confluence. At the upstream cross section, the bed elevation will be deposited about 2 m at the main and tributary channel and the river bed discordance will change from 2.5m at year 2016 to 2m at year 2029. It is also clear from the figure that at year 2029 the reach will be recovered at section eight as same as year 2016. There is some different at bed elevation from years 2016 and 2029. At year 2029 the reach will be deposited at the east bank from section four to section seven about 1 to 2 m, however at section four to section eight will be eroded at the west bank about 1m. It's obvious that the separation zone decreases from year 2016 to 2029.



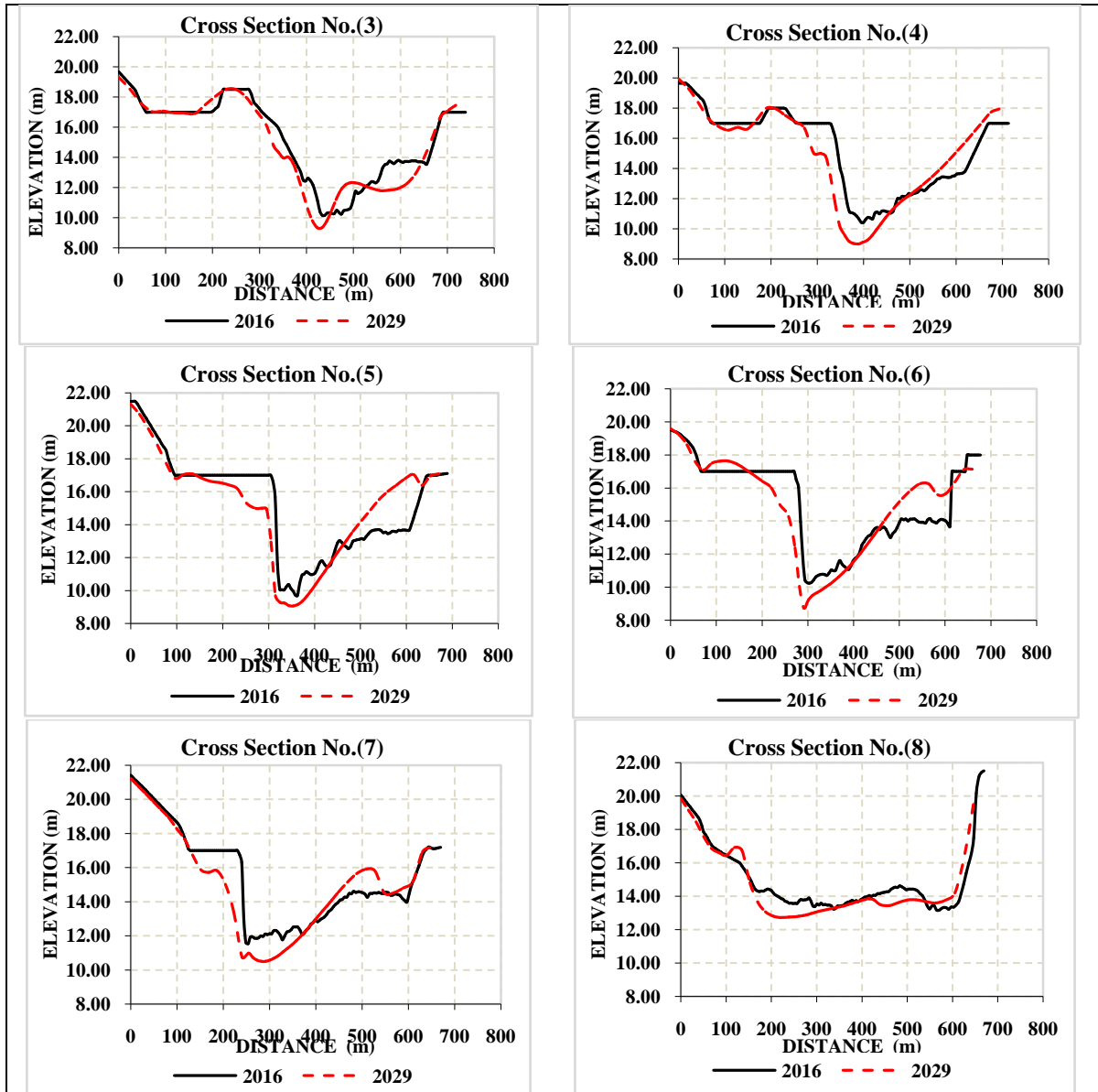


Figure 8: Morphological changes in bed morphology from year 2016 to year 2029

2.2.6 Sedimentation and Erosion Pattern

Figure 9 shows the cumulative erosion and sediment from year 2016 to year 2029. It can be observed that the island will be deposited towards the main channel by rate 0.15 m/year.

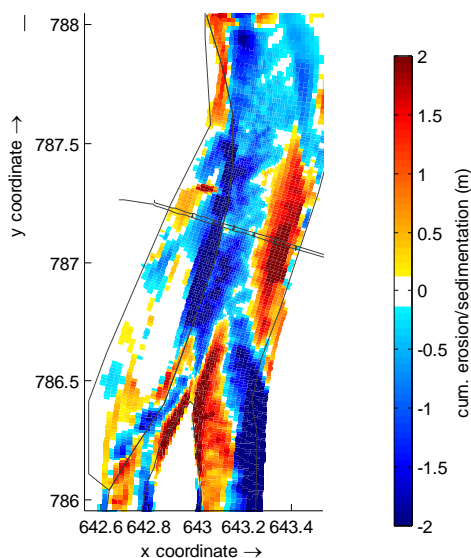


Figure 9: Cumulative erosion and sediment from year 2016 to year 2029

The bed shear stress was estimated for the whole reach at years 2016 & 2029 for maximum flow, figure 10. From the figure it is noticed that the bed shear stress started from the main channel. At year 2016 the bed shear stress reached to 5.5 N/m^2 while at year 2019 it reached to 4.5 N/m^2 . It is noticed also that the value of shear stress reduced at year 2029 compared with year 2016. From the previous part, it means that without human interference the reach will be safer to the bridge in the future from the local scour.

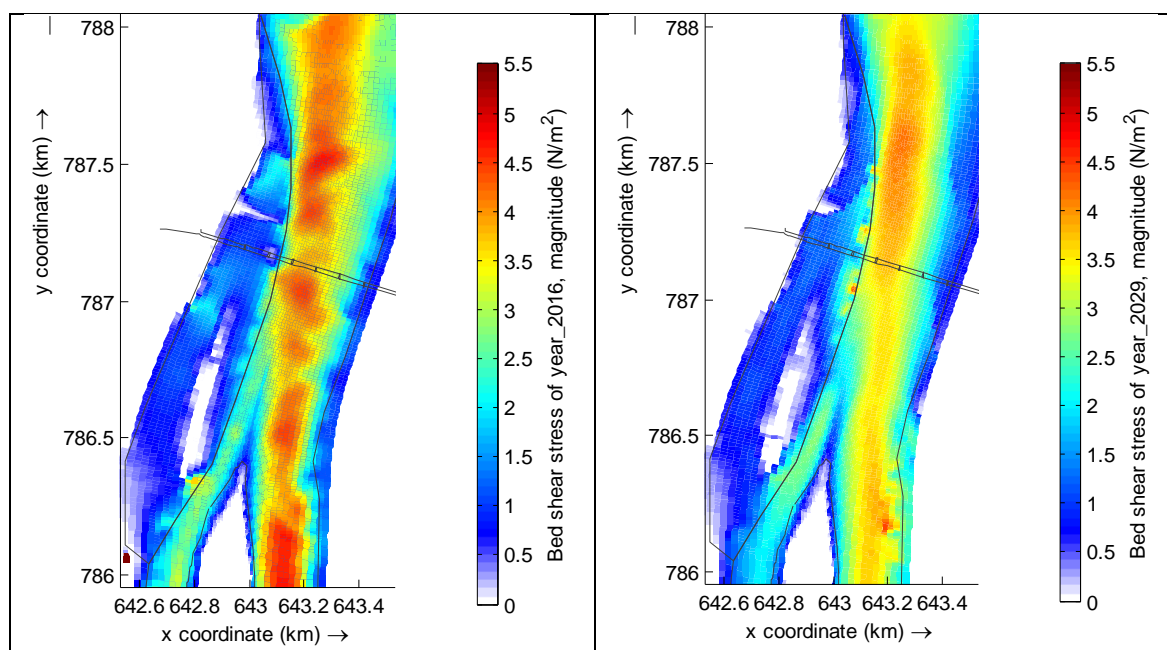


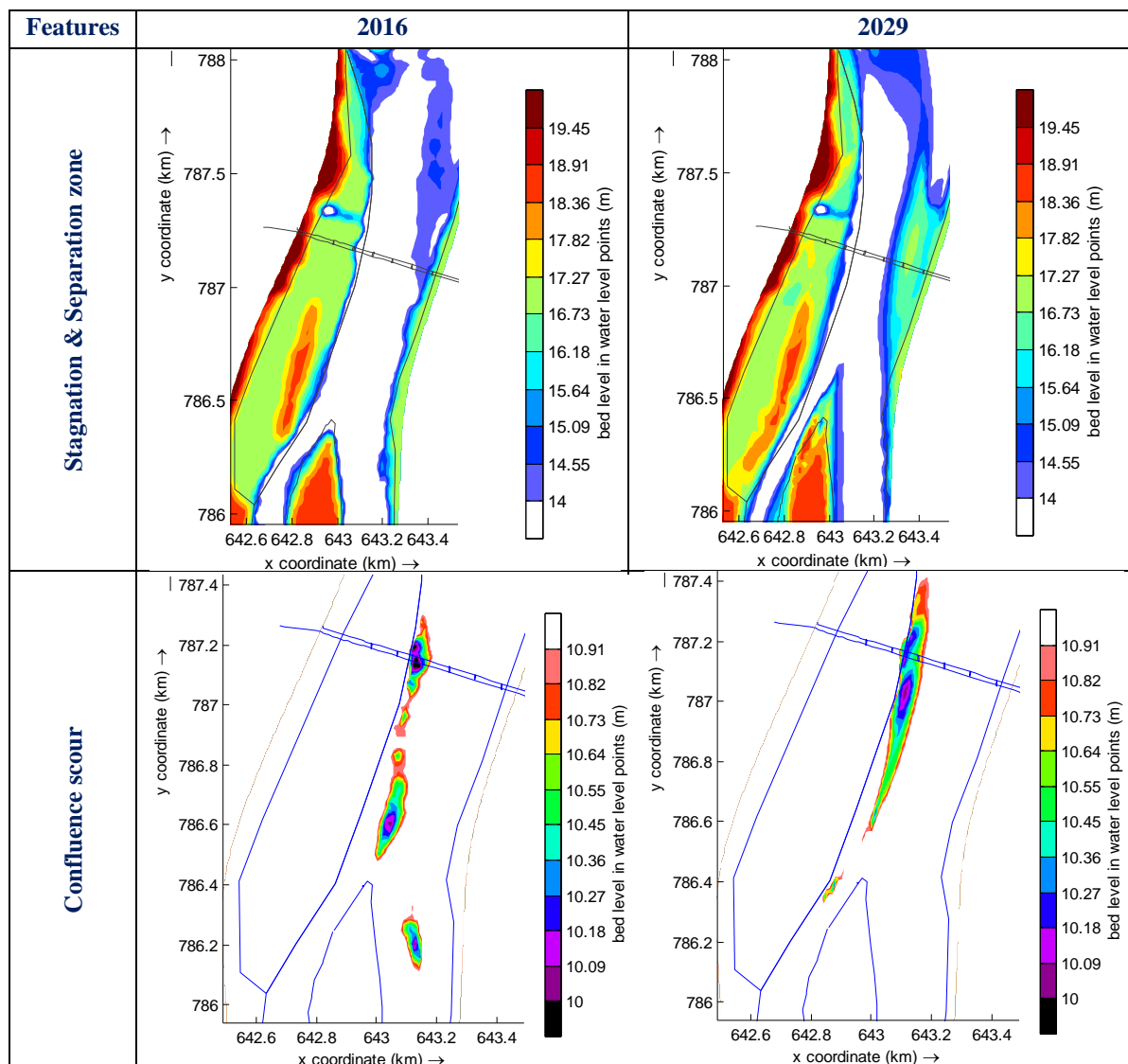
Figure 10: Bed shear stress of maximum flow at years 2016&2029

2.2.7 Hydro-dynamic zones

The hydrodynamic zones at years 2016 and the predicted year 2029 presented at figure 11. From the figure there is changes at the zones would be presented as follows:

- Zone no. 1: the **stagnation zone** will be expanded toward the east side (main channel) subsequently, the confluence angle will be decreased from 25° to 15° .
- Zone no. 2: the **separation zone** will be decrease at year 2029 consequence of the change at the direction of the stagnation zone. The east bank will be deposited about 3 m compared with the bed elevation at year 2016.

- Zone no. 3: the location of the **scour zone** changes from just downstream the confluence at year 2016 to be direct upstream the bridge at about 400 m from the confluence at year 2029.
- Zone no. 4: the **maximum velocity** changes at value and location from year 2016 to 2029. The value will be increase and located downstream the bridge.
- Zone no. 5: the flow will be **recovered** earlier at year 2029 compared with year 2016.
- Zone no. 6: the **mixing shear layer** at year 2029 will be deflected toward the east bank (main channel) and it will be end earlier than year 2016.



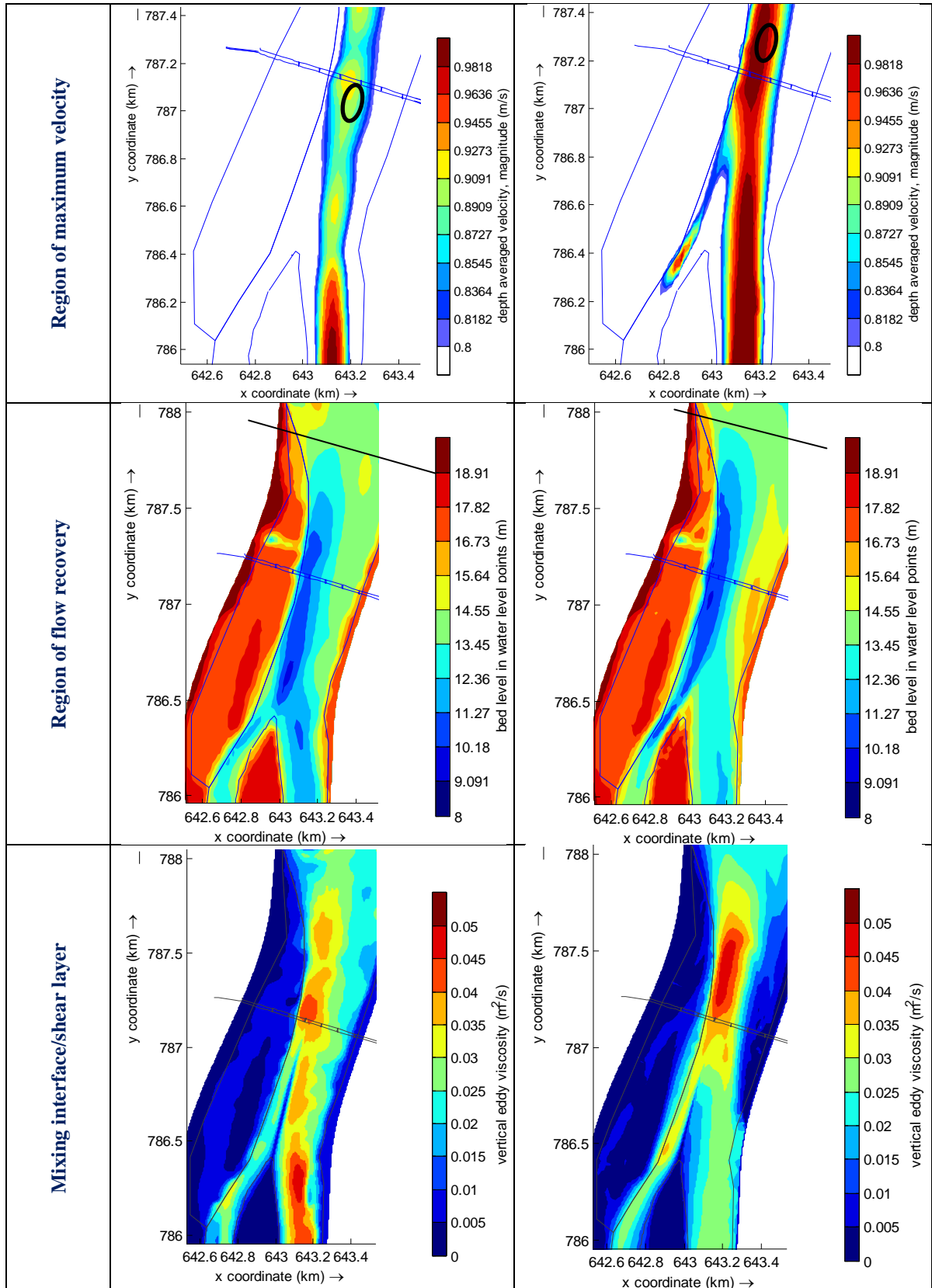


Figure 11: The hydro dynamic features at the confluence zone at year 2016 and 2029

2.2.8 The rate of changes at CHZ

Table 2 and figure 12 presented the changes of distance, value and length of the hydrodynamic zones at year 2016 and the predicted year 2029. The figure shows also the map of key hydrodynamic features observed at years 2016 and 2029.

It can observe that the stagnation zone will be deposited by rate 18.7 m/year, the separation zone length will be expanded about 12.5 m/year while the separation index value will be decreased and the confluence scour will be deposited about 0.08 m/year.

Table 2: Comparing between the hydrodynamic features proports at years 2019 and 2029

Features	Magnitude		Location(m)		Length (m)	
	2016	2029	2016	2029	2016	2029
Stagnation Zone	-	-	-	-	-	244
Separation Index	0.13	0.095	-	-	1890	2057
Confluence Scour	9.88 m	10.91 m	218	411	-	-
Maximum Velocity	0.99 m/s	1.10 m/s	721	640	-	-
Flow Recovery	-	-	1488	1226	-	-
Shear Layer	-	-	-	-	869	387

Where: location= the distance downstream the confluence, Separation index = H/L, where H is maximum separation zone width and L is separation zone length; (Best 1984).

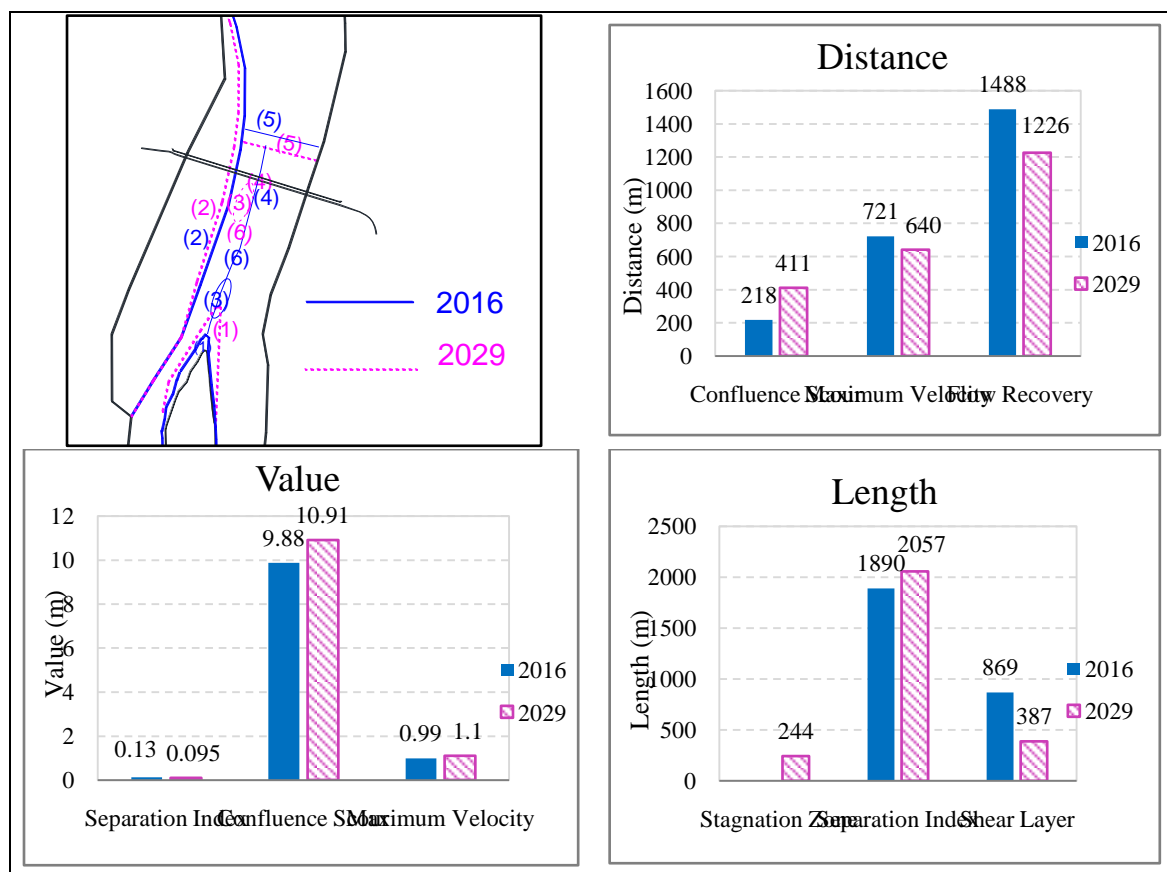


Figure 12: Comparing between the zones proports at years 2019 and 2029

V. CONCLUSIONS

The numerical model is applied to predict flow pattern and morphological changes at the future. The results show the hydro-morpho-sedimentary processes occurring in confluence zone. With a morphological scale factor, the bed-form change of the study confluence is predicted. Interaction between flow dynamics and bed morphology was observed.

The results show that at the future without any human interference, the stagnation zone will be expanded toward the east side, the separation zone will be decrease, the location of the scour zone changes, the

maximum velocity changes at value and location, the flow will be recovered earlier, the mixing shear stress will be ended earlier the erosion and deposition migrate in both directions. So, the results show that the confluence zone will be changes compared with the present time. The different erosion patterns are related to net deflection of flow toward the east bank (main channel) and the consequent acceleration. The spatial distribution of the bed sediments exhibited segregation between the sediments provided by the tributary and main channel.

REFERENCES:

- [1]. Ashmore, P. (1982), Laboratory modelling of gravel braided stream morphology, *Earth Surf. Processes Landforms*, 7, 201– 225.
- [2]. Best, J. L. (1987), Flow dynamics at river channel confluences: Implications for sediment transport and bed morphology, in *Recent Developments in Fluvial Sedimentology*, Spec. Publ. SEPM Soc. Sediment. Geol., 39, 27–35.
- [3]. Best, J. L. (1988), Sediment transport and bed morphology at river channel confluences, *Sedimentology*, 35, 481–498.
- [4]. Best, J. L., and A. G. Roy (1991), Mixing layer distortion at the confluence of unequal depth channels, *Nature*, 350, 411– 413.
- [5]. Biron, P., A. G. Roy, and J. L. Best (1996a), Effects of bed discordance on flow dynamics at open channel confluences, *J. Hydraul. Eng.*, 122, 676–682.
- [6]. Biron, P., A. G. Roy, J. L. Best, and C. J. Boyer (1993a), Bed morphology and sedimentology at the confluence of unequal depth channels, *Geomorphology*, 8, 115– 129.
- [7]. Biron, P., B. De Serres, A. G. Roy, and J. L. Best (1993b), Shear layer turbulence at an unequal depth channel confluence, in *Turbulence: Perspectives on Flow and Sediment Transport*, edited by N. J. Clifford, J. R. French, and J. Hardisty, pp. 197– 213, John Wiley, Hoboken, N. J.
- [8]. De Serres, B., A. G. Roy, P. Biron, and J. L. Best (1999), Three-dimensional flow structure at a river channel confluence with discordant beds, *Geomorphology*, 26, 313–335.
- [9]. DELTARES (2014a) Delft3D-FLOW User Manual; Simulation of multi-dimensional hydrodynamic flows and transport phenomena, including sediments. Version 3.15.34158, Delft.
- [10]. Gaudet, J. M., and A. G. Roy (1995), Effect of bed morphology on flow mixing length at river confluences, *Nature*, 373, 138– 139.
- [11]. Hussain, A. K. M. F., and K. B. M. Q. Zaman (1985), An experimental study of organized motions in turbulent plane mixing layer, *J. Fluid Mech.*, 159, 85–104.
- [12]. Lee, L. H. Y., and J. A. Clark (1980), Angled injection of jets into a turbulent boundary layer, *Trans. AMSE*, 102, 211 –218.
- [13]. McLelland, S. J., P. J. Ashworth, and J. L. Best (1996), The origin and downstream development of coherent flow structures at channel junctions, in *Coherent Flow Structures in Open-Channel Flows*, edited by P. J. Ashworth et al., pp. 459– 490, John Wiley, Hoboken, N. J.
- [14]. Mosley, P. (1976), An experimental study of channel confluences, *J. Geol.*, 84, 535– 562.
- [15]. Nezu, I., and H. Nakagawa (1993), Turbulence in Open-Channel Flows, 281 pp. Int. Assoc. for Hydraul. Res., Madrid, Spain.
- [16]. Reid, I., J. L. Best, and L. E. Frostick (1989), Floods and flood sediments at river confluences, in *Floods: Hydrological, Sedimentological and Geomorphological Implications*, edited by K. Beven and P. A. Carling, pp. 135– 150, John Wiley, Hoboken, N. J.
- [17]. Rhoads, B. L., and A. Sukhodolov (2001), Field investigation of threedimensional flow structure at stream confluences: part I. Thermal mixing and time-averaged velocities, *Water Resour. Res.*, 37, 2393– 2410.
- [18]. Rhoads, B. L., and A. Sukhodolov (2004), Spatial and temporal structure of shear-layer turbulence at a stream confluence, *Water Resour. Res.*, 40, 2393– 2410.
- [19]. Rhoads, B. L., Johnson, K. K. (2018), Three-dimensional flow structure, morphodynamics, suspended sediment, and thermal mixing at an asymmetrical river confluence of a straight tributary and curving main channel. *Geomorphology* 323, 51-69. <https://doi.org/10.1016/j.geomorph.2018.09.009>
- [20]. Rhoads, B. L., and S. T. Kenworthy (1995), Flow structure at an asymmetrical stream confluence, *Geomorphology*, 11, 273– 293.
- [21]. Sukhodolov, A., and B. L. Rhoads (2001), Field investigation of three-dimensional flow structure at stream confluences: 2. Turbulence, *Water Resour. Res.*, 37, 2411– 2424.
- [22]. Winant, C. D., and F. K. Brownand (1974), Vortex pairing: The mechanism of turbulent mixing layer growth at moderate Reynolds number, *J. Fluid Mech.*, 63, 237– 255.